Journal of the Civil Engineering Forum, September 2026, 12(3):293-304
DOI 10.22146/jcef.26551
Available Online at https://jurnal.ugm.ac.id/v3/jcef/issue/archive

Effect of Relative Density Variation on The Effectiveness of Fly Ash in Stabilization of Sandy Soils for Liquefaction Mitigation

Yunan Yakuta Wangsawitana[1], Muhammad Fauzan[1], Heriansyah Putra[1,*], Erizal[1], Minson Simatupang[2]
[1]Department of Civil and Environmental Engineering, IPB University, Bogor, INDONESIA
[2]Departement of Civil Engineering, Halu Oleo University, Kendari, INDONESIA
*Corresponding author: heriansyahptr@apps.ipb.ac.id

SUBMITTED 28 November 2025 **REVISED** 02 February 2026 **ACCEPTED** 23 February 2026

ABSTRACT Indonesia is highly vulnerable to earthquakes that can trigger soil liquefaction, particularly in coastal regions where saturated sandy soils with low relative densities are prevalent. This study investigated the influence of varying Class C fly ash contents (5%, 10%, and 15%), relative densities (50%, 70%, and 90%), and curing periods (7 and 14 days) on the unconfined compressive strength of fully saturated sandy soils as a liquefaction mitigation approach. The methodology included physical soil characterization, sample preparation with specific fly ash and relative density variations, and unconfined compressive strength testing after the curing period. The results demonstrated that increasing the fly ash content, relative density, and curing time significantly enhanced the strength of the samples. The highest strength occurred at 15% fly ash and 90% relative density, with 426.22 kPa (7 days) and 438.57 kPa (14 days). The most notable improvement occurred with an increase in fly ash content from 5% to 10% and relative density from 50% to 70%. Fly ash was more effective at enhancing the strength of sandy soil by promoting interparticle cementation, whereas excessive compaction tended to disrupt the soil structure and generate fine particles that reduced cohesion, as evidenced by the UCS test results and SEM observations. The most significant strength gain between 7 and 14 days was observed at 50% relative density and 5% fly ash, with a twofold increase. The combination of 10% fly ash and 70% relative density was optimal for field implementation, as it yielded strength values exceeding the liquefaction resistance thresholds, while maintaining practical compaction levels and material efficiency. A comparative cost assessment considering materials, labor, equipment, and construction time is recommended to evaluate the practical feasibility of fly ash stabilization relative to alternative ground improvement methods for Indonesian projects.

KEYWORDS Fly Ash; liquefaction; relative density; saturated sand; UCS.

© The Author(s) 2026. This article is distributed under a Creative Commons Attribution-ShareAlike 4.0 International license.

1 INTRODUCTION

Indonesia is situated at the convergence of four active global tectonic plates: the Indo-Australian, Eurasian, Philippine, and Pacific plates. This geotectonic setting renders the country highly susceptible to seismic activity (Ministry of Public Works and Public Housing (PUPR), 2022). One of the significant consequences of earthquakes is the loss of soil strength owing to the intensity and duration of ground shaking, potentially leading to liquefaction. This risk is especially relevant in coastal regions like Indonesia, where saturated sandy soils commonly exhibit low relative densities and high void ratios (Sholihah et al., 2019).

Furthermore, tidal fluctuations can influence the bearing capacity of sandy coastal soils, increasing their vulnerability to liquefaction under saturated conditions (Adinda et al., 2019). Tidal cycles can elevate the groundwater level and reduce the initial effective stress in sandy soils, thereby increasing their susceptibility to excess pore-water pressure. Nevertheless, the development of excess pore water pressure during seismic events is primarily governed by earthquake-induced cyclic loading, while tidal fluctuations mainly act as a preconditioning factor that brings the soil closer to a critical stress state rather than serving as the principal cause of liquefaction (Dong et al., 2022).

Liquefaction frequently occurs when the shear strength of soil is significantly reduced owing to continuous shaking, particularly during earthquakes (Anidhea and Suliyanah, 2021). According to the Indonesian Agency for Meteorology, Climatology, and Geophysics (BMKG), the magnitude 7.4 tectonic earthquake that struck 26 km north of Donggala Regency, Central Sulawesi, on September 28, 2018, triggered a tsunami along the western coast of Sulawesi Island with waves reaching nearly 6 m in height. This event was followed by widespread liquefaction, which caused the soil to lose its load-bearing capacity, leading to ground failure, tilting, subsidence, and structural collapse.

Liquefaction typically affects saturated sandy soils with

low relative densities, resulting in a saturation ratio of 100% (S_r = 100%) (Laia, 2015). In fully saturated soils, all void spaces are filled with water; under loading, this leads to increased pore water pressure. An elevated pore pressure reduces the effective stress, which in turn decreases the shear strength of the soil. This risk is further exacerbated in loose sandy soils, which often exhibit relative densities below 50% (Legrans, 2016). At even higher densities (>70%), sands remain compact and retain shear strength under excess pore pressure, with a relative density (D_r) of 90% sands demonstrating significantly greater resistance to liquefaction owing to stronger interparticle contact and internal friction (Bensoula et al., 2022; Pratiwi, 2020).

Various soil stabilization methods have been developed to mitigate liquefaction, including the use of fly ash, a coal combustion byproduct. Fly ash possesses pozzolanic properties, reacting with water and calcium hydroxide to form strong calcium silicate hydrates (CSH), enhancing soil strength, stiffness, and reducing permeability. Two main types of fly ash, Class C and Class F, are typically used in soil stabilisation. Class F fly ash contains low CaO (<10%) and is purely pozzolanic, requiring lime activation to induce cementitious behaviour (Nurdiyanto et al., 2024). Aydilek and Arora (2005) demonstrated that sandy soils stabilised with 40% Class F fly ash and lime exhibited increased unconfined compressive strength (UCS) from 300 kPa to 400 kPa over curing time. However, this also results in decreased plasticity. Cristelo et al. (2011) found that Class F fly ash activated with sodium silicate and sodium hydroxide produced lower UCS values than cement-based mixtures, requiring prolonged curing times (28–365 days) to achieve significant strength gains (7000–43500 kPa at 40% fly ash).

Class C fly ash contains a higher CaO content (8–20%) and possesses pozzolanic and cementitious properties, enabling self-cementation (Rahmayanti et al., 2023). Simatupang et al. (2020) investigated the mechanical behaviour of Pohara sand stabilised with 5–30% Class C fly ash under relative density of 50% and curing periods of 7–56 days across various saturation levels. Their findings indicated increased UCS and shear strength with increasing fly ash content and decreasing fly ash saturation. The highest UCS and shear strength values under S_r = 100% were obtained with 30% fly ash: 17.95 kPa and 326.56 kPa, respectively, attributed to the binding effect of fly ash particles forming larger, more cohesive agglomerates.

Subsequent work by Simatupang et al. (2022) further confirmed the tensile strength enhancement in sandy soils stabilized with 5–20% Class C fly ash at varying saturation levels. The highest splitting tensile strength (10 kPa) was recorded for 20% fly ash under 30% saturation after 28 days of curing. The strength gain was attributed to the pozzolanic activity, cementation, and hardening, which were more effective at lower saturation. These findings confirm the superior performance of Class C over Class F fly ash.

Yazici and Unsever (2024) reported that stabilizing fine sand (D_r 80%) with 3% cement and 5–25% Class C fly ash over 7–28 days resulted in the maximum friction angle increase at 5–10% fly ash (3.53%, from 47.82° to 49.51°). Similarly, Febrian et al. (2024) found that 10–15% Class C fly ash with 7-day curing enhanced the shear strength by 22.9% (from 9.53 to 11.71 kPa), whereas increasing the dosage to 20% produced only marginal improvement. Turan et al. (2020) also observed that 10–15% fly ash with 7-day curing yielded the highest UCS increase of 30.56% (from 372.6 kPa to 486.4 kPa). SEM observations by Dissanayake et al. (2017) indicated that fly ash contents above 16% resulted in an abundance of unreacted particles, thereby limiting effective cementitious bonding. Although a higher fly ash content generally increases strength, the rate of improvement diminishes beyond the optimum dosage owing to reduced reaction efficiency and possible matrix disruption. Therefore, 5%, 10%, and 15% Class C fly ashes were selected as the effective stabilization ranges in this study. In addition to its technical effectiveness, fly ash stabilization offers economic advantages over conventional liquefaction mitigation methods, such as stone columns and deep soil mixing. As an industrial byproduct, fly ash is generally more cost-effective because of its lower material costs and reduced construction complexity, while simultaneously contributing to waste utilization and environmental sustainability (Gupta et al., 2024; Karthikeyan and George, 2023).

While previous studies have confirmed the beneficial effects of Class C fly ash in improving the strength of sandy soils, most have been restricted to partially saturated conditions and have not simultaneously examined the influence of relative density and fly ash dosage under full saturation. Under S_r = 100%, sandy soils exhibit very low undrained shear strength and are highly susceptible to flow failure (Zeybek and Madabhushi, 2017). Achieving fully saturated conditions in laboratory settings poses challenges due to the potential presence of occluded air within the pore spaces (Sakaguchi et al., 2005). To mitigate this issue, a controlled addition of water based on the calculated pore volume (V_v), along with sealed curing and stringent control of dry unit weight, was employed to ensure consistent relative density throughout specimen preparation and testing.

This study aims to evaluate the effectiveness of Type C fly ash in stabilizing fully saturated sandy soils (S_r = 100%) under three relative densities (50%, 70%, and 90%) using fly ash contents of 5–15%, with strength behaviour assessed through unconfined compressive strength (UCS) testing. The findings are expected to

provide new insights into the interaction between saturation, fly ash dosage, and relative density, offering a scientific basis for the application of fly ash as a practical liquefaction mitigation strategy.

2 METHODS

2.1 Material

The soil sample used in this study was classified as Bangka sand. The specific gravity (G_s) of the sample was 2.53, which fell within the standard range of 2.4–2.7, as specified by ASTM C 128-07a, indicating that the material was consistent with typical sand properties (American Society for Testing and Materials, 2009). The minimum void ratio (e_{min}) reflects the densest packing condition of sand (0.41–1.0), whereas the maximum void ratio (e_{max}) represents its loosest state (0.6–1.2) (Briaud, 2013). Laboratory testing yielded a minimum void ratio (e_{min}) of 0.46 and a maximum void ratio (e_{max}) of 0.81.

The particle size distribution curve (Figure 1) produced characteristic diameters of D_{10} = 0.24 mm, D_{30} = 0.51 mm, and D_{60} = 1.06 mm. The calculated uniformity and gradation coefficients were C_u = 4.42 and C_c = 1.01, respectively, classifying the soil as poorly graded sand (SP) under the USCS (ASTM D2487-11) (American Society for Testing and Materials, 2011). Poorly graded sand is highly susceptible to liquefaction under increased pore-water pressure. Plotting the grading curve on the Tsuchida liquefaction potential chart confirmed its location within the liquefaction susceptibility zone (Koester and Tsuchida, 1988).

According to Koester and Tsuchida (1988), soil is considered to have liquefaction potential if D_{10} falls within the range of 0.01 mm < D_{10} < 1.00 mm, and high liquefaction potential if 0.04 mm < D_{10} < 0.30 mm. The D_{10} value obtained in this study was 0.24 mm, indicating a high liquefaction potential. This relatively low D_{10} value is associated with an increased presence of fine

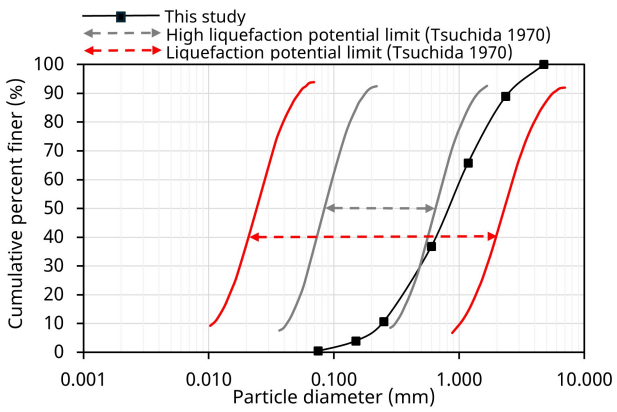

Figure 1. Liquefaction potential curve based on soil grain size.

particles, which reduces the coefficient of permeability of the soil and promotes the buildup of excess pore water pressure under dynamic loading conditions (Lestari, 2022).

2.2 Experiment Design

Three parameters were varied in this study: relative density, fly ash content, and curing time. The relative densities (50%, 70%, and 90%) represented loose, medium, and dense sand conditions, respectively (Frempong and Shukla, 2018). The target relative densities (D_r) were achieved by controlling the dry unit weight (γ_d) of each specimen. The maximum and minimum void ratios (e_{max} and e_{min}) were determined, and the corresponding target dry unit weights (γ_d) were calculated using the standard relative density equation. The required mass of dry sand was then placed into the mold in layers and compacted to the predetermined height to ensure that the target dry unit weight was achieved.

Fly ash contents (5%, 10%, and 15%) were selected based on previous studies showing significant strength improvement within this range (Febrian et al., 2024; Turan et al., 2020). The fly ash dosage was controlled by determining the specific gravity and void ratios of each mixture to calculate its actual void ratio. From the mold volume (V_{mould}) and the volume of solids (V_s), the dry weight of solids (W_s) and pore volume (V_v) were calculated. The dry weight of solids (W_s) represented the combined proportion of sand and fly ash, with 5%, 10%, and 15% fly ash measured relative to the dry weight of sand and homogenized thoroughly before compaction.

Curing durations of 7 and 14 days were selected because the peak early age strength of Class C fly ash-stabilized soils typically occurs within this period (Misra, 1998). Turan et al. (2022) reported that Class C fly ash exhibits greater strength enhancement than Class F fly ash due to its higher CaO content, which promotes both hydraulic and pozzolanic reactions. The elevated calcium content promotes rapid formation of cementitious products, particularly calcium silicate hydrate (C–S–H) and calcium aluminate hydrate (C–A–H) (Dissanayake et al., 2017; Yazici and Unsever, 2024).

UCS testing was selected because it effectively evaluates the bonding and cementation effects of calcium-rich fly ash in sandy soils (Kolias et al., 2005). Previous research has indicated that a UCS value of approximately 98 kPa may represent an indicative lower-bound strength associated with reduced liquefaction susceptibility in sand (Zen et al., 1998). Therefore, the UCS values obtained at 7 and 14 days were compared with this reference level to assess the effectiveness of strength development over the curing time.

Table 1. Variations of test samples

Test Samples	Concentration		Treatment
	D_r (%)	Fly ash (%)	
A01		5	
A02	50	10	
A03		15	
B01		5	
B02	70	10	S_r = 100% Curing 7 and 14 days
B03		15	
C01		5	
C02	90	10	
C03		15	

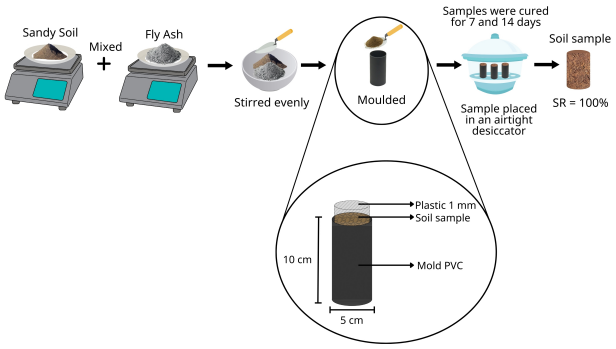

Figure 2. Schematic of test sample preparation.

Full saturation (S_r = 100%) was achieved by filling the calculated pore volume (V_v) with water. The verification and preservation of S_r = 100% were ensured by lining each mold with plastic and storing it in a sealed container or desiccator during curing to maintain 100% humidity and to prevent moisture loss. Three specimens were prepared for each parameter combination, yielding 27 samples per curing period, for a total of 54 samples. Each specimen was tested, and the average UCS value was used for the analysis, whereas the standard deviation assessed the data variability. For microstructural investigation, selected specimens were oven-dried before SEM analysis to eliminate free moisture and preserve the internal microstructure for accurate imaging. The detailed combinations of parameters and corresponding sample quantities are listed in Table 1.

2.3 Specimen Preparation

The sand–fly ash mixture samples were prepared using cylindrical PVC moulds with a height of 10 cm and a diameter of 5 cm, following the standard procedure for unconfined compressive strength (UCS) testing of sandy soils. Before sample placement, the moulds were positioned vertically and lined with plastic wrap. This lining facilitated the demolding process after compaction and preserved the cylindrical shape of the specimen, thereby preventing surface damage during the extraction. The test specimens, consisting of sand mixed with varying percentages of fly ash under different relative density (D_r) conditions, were compacted into moulds using the layer compaction method.

The specimens were compacted into five equal layers to achieve target relative densities (D_r) of 50%, 70%, and 90%, with the compaction effort adjusted according to the procedure reported by Simatupang et al. (2020). Each layer was subjected to 15, 25, and 40 uniformly distributed blows to attain loose (D_r 50%), medium dense (D_r 70%), and dense (D_r 90%) conditions, respectively. Compaction was performed manually using a laboratory rubber mallet, which was raised approximately 5 cm above the soil surface prior to each blow.

During this process, the interaction between sand and Class C fly ash was critical to the integrity of the specimen. The high CaO content triggered hydration, forming C–S–H and C–A–H compounds that bonded, coated, and bridged particles, filled voids, and enhanced interparticle cementation, allowing the mixture to maintain its cylindrical shape after demoulding (Kolias et al., 2005; Siddique, 2004; Transportation Research Board, 1986). The samples were subsequently cured for 7 and 14 days after compaction. UCS testing was conducted to evaluate the influence of relative density on the mechanical behavior of fly ash-stabilized sand. A schematic illustration of the sample preparation procedure using cylindrical moulds is presented in Figure 2.

2.4 Test Method

The unconfined compressive strength (UCS) test was conducted using SNI 3638:2012 on the Method of Unconfined Compression Test for Cohesive Soils (National Standardization Agency of Indonesia, 2012). Although the Unconfined Compressive Strength (UCS) test does not directly capture cyclic behavior, increases in UCS enhance undrained shear strength and stiffness, thereby indirectly improving cyclic resistance and indicating a reduced susceptibility to liquefaction (Park et al., 2025). After compaction and curing for 7 or 14 days in a sealed container, the specimens were carefully demoulded from the PVC moulds by gradually pulling the plastic lining upward in the axial direction to avoid end damage. The height and diameter of each specimen were measured using a vernier caliper with an accuracy of ±0.1 mm.

The test was performed by placing the cylindrical specimen on the lower platen of the compression testing machine. The upper platen was then adjusted to contact the top surface of the specimen. Before loading, the deformation indicator was set to zero to ensure accurate displacement measurements. The load was applied vertically from below, activating both the load and displacement gauges, thereby allowing displace-

ment data to be acquired throughout the test. Loading was continued until the initial signs of failure were observed, such as the appearance of cracks or a significant drop in the peak load. This procedure aimed to capture the maximum axial load that the specimen could withstand without complete structural failure. A schematic of the UCS testing setup is shown in Figure 3.

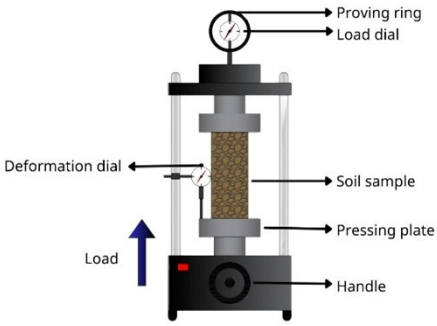

Figure 3. Schematic of uniaxial compressive strength testing with UCS apparatus.

Scanning Electron Microscopy (SEM) was employed to characterize the microstructural morphology by examining the interaction of a high-energy electron beam with the sample surface to produce high-resolution images (Temiz, 2022). This technique enables the visualization of hydration products, such as calcium-silicate-hydrate (C–S–H) and calcium-aluminate-hydrate (C–A–H) phases generated from pozzolanic reactions between fly ash and cementitious constituents, as well as textural features, including sand particles, fly ash particles, pore networks, and microcracks in the matrix (Chyliński, 2024) SEM observations were conducted at a magnification of 1000× and an accelerating voltage of 15 kV to ensure an appropriate resolution for microstructural assessment.

3 RESULTS

3.1 Material Characteristics

The characterization of the sand–fly ash mixtures was conducted following standard procedures used for natural soils. The specific gravity of the fly ash, the specific gravity of sand–fly ash mixtures, and the void ratio of each mix were determined. These parameters are essential for determining the appropriate proportions of sand, fly ash, and water during sample preparation. The fly ash used in this study was classified as Class C, with a measured specific gravity (G_s) of 2.87. This value falls within the generally reported range of 2.15–2.80 (Mehta, 2004), while broader ranges of 1.6–3.1 have also been reported (Ulum, 2014).

The specific gravities of the sand–fly ash mixtures with 5%, 10%, and 15% fly ash were measured as 3.02, 3.40, and 3.55, respectively. Theoretical specific gravities, calculated using a weighted average of sand and fly ash contents, were 2.55, 2.56, and 2.58, respectively. This testing followed SNI 1964:2008 on the Determination of Soil Specific Gravity (National Standardization Agency of Indonesia, 2008), with kerosene used as the medium instead of water because fly ash can react with water, as also reported by Annisa and Widayanti (2025). The specific gravities obtained from the tests were higher than the theoretical values obtained from the literature. This discrepancy is attributed to the use of kerosene in the sand–fly ash mixtures, which has a lower density and different adhesion properties than water (Andariana et al., 2024).

Table 2. Properties of test sample variations

FA (%)	G_s	e_{max}	e_{min}	e_{50}	e_{70}	e_{90}
5	3.02	1.11	0.75	0.93	0.86	0.79
10	3.40	1.43	0.96	1.19	1.10	1.01
15	3.55	1.57	1.06	1.31	1.21	1.11

The minimum (e_{min}) and maximum (e_{max}) void ratios were determined for each mixture and used to calculate the actual void ratio at relative densities (D_r) of 50% (e_{50}), 70% (e_{70}), and 90% (e_{90}). The results are summarized in Table 2.

As the fly ash content increased, the actual void ratio at each relative density (D_r) level also tended to increase. This is due to the characteristics of fly ash, which contains larger air voids than typical soils. According to Upadhyay et al. (2007), fly ash exhibits air voids ranging from 5% to 15%, whereas soils generally have approximately 1% to 5% under maximum density conditions. Furthermore, some fly ash particles are hollow or internally porous, thereby contributing additional voids to the overall soil–fly ash system (Yadav et al., 2021).

3.2 Effect of Fly Ash Concentration

The unconfined compressive strength (UCS) test results for each variation in fly ash content and relative density are illustrated in Figure 4, with detailed numerical values presented in Table 3.

At 7-day curing, the highest UCS values were recorded at D_r 90% for 5%, 10%, and 15% fly ash contents, with corresponding values of 65.53 kPa, 206.67 kPa, and 426.22 kPa, respectively. Similarly, at 14-day curing, the maximum UCS values were also observed at D_r 90% for 5%, 10%, and 15% fly ash, with values of 69.27 kPa, 306.97 kPa, and 438.57 kPa, respectively. This increasing trend was also observed for D_r 70% and D_r 50%, although the latter consistently exhibited the lowest UCS values. Notably, adding fly ash from 5% to 10% resulted in a more substantial improvement in the UCS than the increase from 10% to 15% across all relative

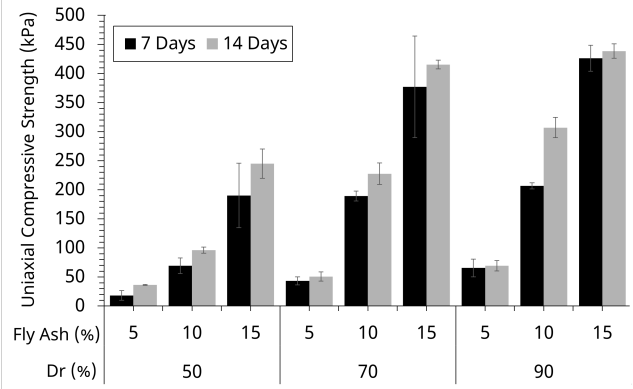

Figure 4. Unconfined compressive strength (UCS) in relation to varying fly ash content.

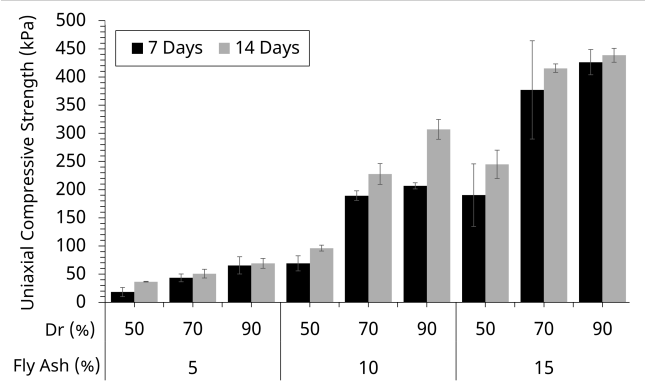

Figure 5. Unconfined compressive strength (UCS) in relation to varying relative density.

Table 3. UCS values of sand samples with varying fly ash content and relative density

Fly Ash (%)	D_r (%)	UCS (7 days)	UCS (14 days)
	50	18.26	36.53
5	70	43.36	50.82
	90	65.53	69.27
	50	69.23	96.07
10	70	189.25	227.58
	90	206.67	306.97
	50	190.23	244.83
15	70	377.03	415.41
	90	426.22	438.57

density levels. The most pronounced strength gain due to this 5–10% increment occurred at D_r 70%, where UCS values increased by approximately 4.4 times at 7-day curing (from 43.36 kPa to 189.25 kPa) and 4.5 times at 14-day curing (from 50.82 kPa to 227.58 kPa), compared to other D_r.

3.3 Effect of Relative Density

The unconfined compressive strength (UCS) values increased with increasing relative density across all combinations of fly ash content and curing duration. The UCS values for each relative density level are shown in Figure 5.

At 7-day curing, the highest strength was obtained with 15% fly ash content at D_r of 50%, 70%, and 90%, with corresponding UCS values of 190.23 kPa, 377.03 kPa, and 426.22 kPa, respectively. A similar trend was observed for the 14-day curing period, with UCS values of 244.83 kPa, 415.41 kPa, and 438.57 kPa for D_r 50%, 70%, and 90%, respectively. Although lower strength values were recorded at 10% and 5% fly ash, the same increasing trend with the D_r was maintained. As presented in Figure 5, an increase in relative density from 50% to 70% led to a more substantial improvement in UCS than an increase from 70% to 90% across all fly ash contents. The most notable gain from 50% to 70% was observed at 10% fly ash, with UCS values increasing by 2.73 times at 7-day curing (from 69.23 kPa to 189.25 kPa) and 2.37 times at 14-day curing (from 96.07 kPa to 227.58 kPa), surpassing the improvement observed at other fly ash levels.

Moreover, as shown in Figure 5, the curing duration (7 vs. 14 days) significantly affected the UCS improvement. At D_r 50%, the highest UCS gain from 7 to 14 days was observed at 5% fly ash, with a twofold increase, followed by 10% and 15% fly ash with increases of 1.39 and 1.29 times, respectively. At D_r 70%, the most significant gain occurred at 10% fly ash (1.20 times), followed by 5% (1.17 times) and 15% (1.10 times). For D_r 90%, the highest increase was also recorded at 10% fly ash (1.49 times), followed by 5% (1.06 times) and 15% (1.03 times).

4 DISCUSSION

4.1 Material Characteristics

The specific gravity of the fly ash used in this study was relatively high (2.87). A higher specific gravity is generally associated with a more complex physical texture, which is attributed to variations in coal sources and combustion processes (Gunawan and Nono, 2019). The specific gravity of the sand–fly ash mixtures exhibited an increasing trend with increasing fly ash content. In practice, the measured specific gravity values were consistently higher than those obtained from theoretical calculations. As shown in Table 3, an increase in the D_r corresponded to a decrease in the void ratio. This reduction in porosity reflects an increase in soil compactness, which reduces void spaces within the soil matrix (Pangaribuan et al., 2020). Moreover, the actual void ratio at each D_r tended to increase with higher fly ash content. This can be attributed to the physical characteristics of fly ash, which typically contains more internal air voids than natural soil. A previous study

by Upadhyay et al. (2007) suggested that fly ash particles may exhibit internal voids ranging from 5–15%, whereas soils generally have air voids from 1–5% under maximum compaction conditions.

4.2 Effect of Fly Ash Concentration

The strength improvement of sandy soil in this study is attributed to the characteristics of Class C fly ash, which contains a high percentage of calcium oxide CaO along with reactive silicate and aluminate compounds, such as SiO_2, Al_2O_3, and Fe_2O_3. These compounds react with water to form calcium hydroxide ($Ca(OH)_2$), which dissociates in water, releasing OH^- ions. This creates an alkaline environment that facilitates the dissolution of SiO_2 and Al_2O_3, leading to the formation of calcium silicate hydrate (C–S–H) and calcium aluminate hydrate (C–A–H) compounds (Kolias et al., 2005; Transportation Research Board, 1986). These hydration products fill soil pores, improve particle gradation, reduce plasticity, and effectively bind soil particles (Siddique, 2004). These bonding agents strengthen the interparticle contact between sand grains, enhancing soil cohesion and internal friction (Pandian, 2004). In addition, fly ash contributes to partial water absorption within the mixture, coating and binding the soil particles. As a result, even under fully saturated conditions (S_r = 100%), the mixture does not experience excess free water that would otherwise weaken the soil structure; instead, it undergoes densification, enhancing its stability.

The increase in fly ash content from 5% to 10% promoted more effective pozzolanic reactions, particularly the formation of calcium silicate hydrate (C–S–H), which enhanced soil cohesion and shear strength, with peak efficiency observed at 10% fly ash (Golewski, 2022). This result suggests that the optimum improvement in unconfined compressive strength (UCS) was achieved at 10% fly ash content. Beyond this optimum content (10% fly ash), the excess fly ash particles no longer act effectively as pore fillers but behave as inert particles. Dissanayake et al. (2017) stated that surplus fly ash can become passive and fail to participate in pozzolanic reactions. Additionally, excessive fly ash increases the total pore volume, disrupting the formation of adequate particle bonding (Osok et al., 2023). These findings indicate that once the optimum fly ash content is exceeded, additional fly ash no longer contributes actively to pozzolanic product formation, particularly the generation of calcium silicate hydrate (C–S–H). The addition of lime or cement to fly ash may activate these otherwise passive particles by providing additional Ca^{2+} and alkalinity, thereby potentially promoting pozzolanic reactions and improving the mechanical strength of the soil (Di Sante et al., 2025).

4.3 Effect of Relative Density

Increasing the relative density of sandy soil results in a tighter particle arrangement and stronger interlocking among grains Igwe (2018). According to Mahvash et al. (2017), a denser particle distribution enhances the contact between fly ash and sand particles, allowing more effective reactions and the formation of calcium silicate hydrate (C–S–H), thereby improving the interparticle interaction and pozzolanic bonding that reinforces the soil structure. A higher density or lower porosity also increases the shear resistance between particles, enabling the soil to withstand greater loads. This is attributed to reduced voids and enhanced particle contact, which strengthen the soil matrix (Mawlood et al., 2021; Ruiz-Chávez et al., 2022; Santana et al., 2021).

The more significant increase in UCS between low (D_r 50%) and medium (D_r 70%) densities compared to the increase from medium (D_r 70%) to high (D_r 90%) densities indicated that porosity reduction was more prominent at lower density ranges. At a D_r of 70%, sand particles formed a relatively stable structure with limited mobility and enhanced interlocking (Zhang et al., 2023). Consequently, increasing compaction to D_r 90% resulted in a shorter densification process and a faster stress peak, limiting the strength improvement due to the density increase. Therefore, the UCS gain from D_r 70% to 90% was less pronounced than that from D_r 50% to 70%. These findings indicate that the most significant rate of strength improvement occurred at a medium relative density, particularly at a D_r of 70%. This finding aligns with that of Herwandi et al. (2017) who reported a more substantial decrease in the sand permeability coefficient at low to medium relative densities.

Interestingly, sand stabilized with 15% fly ash at a D_r of 50% produced a higher UCS than sand with 10% fly ash at a D_r of 70% or 5% fly ash at a D_r of 90%, indicating that increasing fly ash content had a more pronounced effect on strength development than increasing relative density alone. The addition of fly ash is more effective in enhancing the strength of cohesionless sandy soils because fly ash contributes to the chemical bonding among particles. In contrast, increasing the relative density through compaction (e.g., tamping) may damage the existing soil structure, resulting in strength gains that are not proportional to those achieved by fly ash addition. Structural damage from compaction can produce fine particles that fill intergranular voids and behave like silt or clay, reducing cohesion, decreasing permeability, and creating potentially weak zones within the soil mass (Bagheri et al., 2012). Scanning Electron Microscopy (SEM) is essential for examining the microstructure of fly ash-stabilized sand, including pore distribution, particle contacts, and reaction products. This analysis elucidates the mechanisms by which fly ash contributes more effectively to strength devel-

opment than compaction alone.

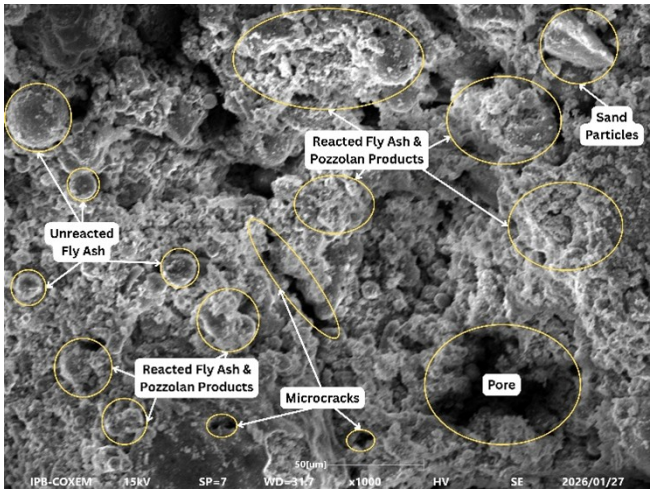

Figure 6. SEM analysis of microstructural characteristics of fly ash-stabilized sand

SEM observations at 1000× magnification of the specimen containing 15% fly ash at a D_r of 50% indicate that strength development is primarily governed by chemical bonding rather than mechanical densification. A continuous cementitious matrix formed by the reacted fly ash and pozzolanic products coats the sand grains and bridges the adjacent particles, while discrete spherical particles remain as unreacted fly ash microspheres (Vennapusa and Eluru, 2025). The presence of this chemically bonded network at a relatively low relative density demonstrates that the cohesion enhancement is not solely dependent on densification (Mohsen et al., 2023). Localised pores and microcracks further suggest that excessive compaction may disrupt the cement matrix and reduce effective bonding (Baloochi, 2022).

Strength improvement during curing occurred because fly ash absorbed water and initiated pozzolanic reactions. These reactions produced cementitious compounds, such as calcium silicate hydrate (C–S–H) and calcium aluminate hydrate (C–A–H), which filled the voids and strengthened the interparticle bonds. Over time, this cementation process enhanced cohesion and soil density, significantly increasing the UCS (Marsindi et al., 2022). At D_r 50%, the UCS increase from 7 to 14 days of curing was most significant at 5% fly ash content, with a two-fold increase, followed by 10% and 15% fly ash contents with 1.39 and 1.29 times increases, respectively. This suggests that 5% fly ash by sand weight was the most efficient dosage at low densities over the curing period. A fly ash content exceeding 5% tended to reduce the bonding efficiency, as its finer particles and larger air voids contributed more to porosity in a loosely compacted matrix (Upadhyay et al., 2007). This trend suggests that, in low-density soils, curing allows pozzolanic reactions to develop and strengthen interparticle bonding sufficiently. In contrast, excessive fly ash in a loosely compacted matrix may disrupt these bonds and limit early-age strength development, as reported by Noaman et al. (2022).

At D_r 70%, the highest UCS gain over the 7–14 days curing period occurred at 10% fly ash (1.20 times), followed by 5% (1.17 times) and 15% (1.10 times). At D_r 90%, the highest UCS increase was also recorded at 10% fly ash (1.49 times), followed by 5% (1.06 times) and 15% (1.03 times). These findings confirm that the relative density and curing duration significantly influence the strength performance of fly ash-stabilized sand, with 10% fly ash content emerging as the most effective level for strength optimization.

Increasing the relative density decreases the void ratio, thereby increasing the number of sand particles per unit volume (Darwis, 2018). This condition necessitates a higher fly ash content to form sufficient bonding between particles at a higher D_r. Additionally, at a high D_r ($\geqslant$ 70%), more effective densification helps minimize air voids caused by fine fly ash particles, resulting in a denser microstructure (Turan et al., 2022). Overall, 15% fly ash yielded the lowest UCS increase during the 7–14 day curing period at all D_r. This suggests that excessive fly ash content leads to passive particles that do not significantly contribute to pozzolanic compound formation.

The selection of the optimal relative density and curing duration (7–14 days) for fly ash–stabilized sand should consider strength, constructability, material efficiency, and cost-effectiveness. The highest relative UCS gain during curing was observed at D_r 50% and 5% fly ash, with a two-fold increase. However, the resulting UCS values were relatively low, from 18.26 kPa (7 days) to 36.53 kPa (14 days). Zen et al. (1998) noted that a UCS value exceeding 98 kPa is considered a critical threshold for liquefaction resistance in sandy soils. Based on the test results, D_r 50% sand required 15% fly ash to reach UCS values between 190.23–244.83 kPa, exceeding the liquefaction safety threshold. Meanwhile, D_r 70% and 90% sand only required a minimum of 10% fly ash to achieve UCS values between 189.26–438.57 kPa. Nevertheless, achieving higher D_rs requires more intensive compaction efforts directly related to the equipment type and associated costs (Arumningsih, 2013).

From a practical standpoint, D_r 50% with 15% fly ash may be viable in the field owing to the minimal compaction effort and UCS values above the liquefaction threshold. However, in actual field conditions, the relative density is likely to increase naturally owing to construction activities such as worker foot traffic, heavy equipment movement, or fill placement, rendering the initial D_r 50% condition less representative (Keramatikerman et al., 2017). From a fly ash utilization efficiency perspective, a D_r of 70% with 10% fly ash

is considered optimal, as it yields UCS values above the liquefaction resistance threshold while using less stabilizing material and requiring compaction levels that are still practical in field conditions. Therefore, the most realistic and efficient combination is a D_r of 70% with 10% fly ash.

A cost analysis, including material, labour, and compaction equipment, is essential to determine the most economically viable and technically effective stabilisation strategy. Moreover, based on Government Regulation (PP) No. 22/2021 on the Implementation of Environmental Protection and Management, fly ash is no longer classified as hazardous waste (locally known as *Bahan Berbahaya dan Beracun* or B3). However, its application still requires careful management owing to its potential to accumulate heavy metals in the environment (Government of the Republic of Indonesia, 2021).

5 CONCLUSION

This study investigated the influence of Class C fly ash content, relative density (D_r), and curing time on the unconfined compressive strength (UCS) of sandy soil as part of efforts to improve its resistance to liquefaction. The hypothesis that both fly ash addition and compaction enhance soil strength was confirmed, with fly ash contributing more effectively than density increase alone, as evidenced by the UCS results and the SEM observations. The UCS increased with higher fly ash content and relative density, reaching maximum values of 426.22 kPa (7 days) and 438.57 kPa (14 days) at 15% fly ash and D_r 90%. The most significant improvement was observed when the fly ash content increased from 5% to 10% at a D_r of 70%. The most optimal increase in UCS occurred when D_r increased from 50% to 70%, particularly at a fly ash content of 10%. The optimal condition, balancing strength, material efficiency, and constructability, was achieved at 10% fly ash and D_r 70%, surpassing the liquefaction resistance threshold. From a practical standpoint, this condition represents a level of field compaction effort that is more readily achievable than the high degree of densification required by conventional liquefaction mitigation methods. Compared with techniques such as rapid impact compaction or stone columns, fly ash–based stabilization provides a simpler alternative and offers potential cost advantages over cement- or lime-based stabilization. These findings extend the current understanding of fly ash utilization for sandy soil stabilization, particularly under varying density conditions. However, the study was limited to laboratory-scale UCS testing under controlled moisture and curing conditions; therefore, field-scale validation is recommended for future research to confirm the long-term performance of the fly ash-stabilized sand. A comparative cost assessment considering materials, labor, equipment, and construction time is recommended to evaluate the practical feasibility of fly ash stabilization relative to alternative ground improvement methods for Indonesian projects.

DISCLAIMER

The authors declare no conflict of interest.

REFERENCES

Adinda, B. T. D., Prabowo, A. and Muchtaranda, I. H. (2019), 'Pengaruh perkuatan geotekstil tipe woven gx-50 terhadap keruntuhan pondasi pada pasir pantai dengan variasi kedalaman muka air', *Spektrum Sipil* **6**(1), 23–31.
URL: *https://doi.org/10.29303/spektrum.v6i1.150*

American Society for Testing and Materials (2009), Standard test method for density, relative density (specific gravity), and absorption of fine aggregate (astm c128-78), Technical report, ASTM International, West Conshohocken.
URL: *https://www.astm.org*

American Society for Testing and Materials (2011), Standard practice for classification of soils for engineering purposes (unified soil classification system) (astm d2487-11), Technical report, ASTM International, West Conshohocken.
URL: *https://doi.org/10.1520/D2487-11*

Andariana, O. A., Hasyim, A., Hamsyah, E. F. and Yusuf, M. (2024), 'Pelatihan ipa sederhana bagi peserta didik di pulau bonetambu', *Jurnal Pengabdian Kepada Masyarakat (J-ABDI)* **3**(11), 2279–2288.

Anidhea, N. O. and Suliyanah (2021), Identifikasi karakteristik struktur tanah dan mitigasi bencana likuifaksi di sulawesi tengah, *in* 'Prosiding Seminar Nasional Fisika (SNF)', Surabaya, Indonesia.

Annisa, R. and Widayanti, A. (2025), 'Karakteristik limbah keramik, agregat alam, dan filler fly ash untuk campuran lapis aus asphalt concrete – wearing course (ac-wc)', *Jurnal Media Publikasi Terapan Transportasi* **3**(1), 61–69.
URL: *https://doi.org/10.26740/mitrans.v3n1.p61-69*

Arumningsih, D. (2013), 'Biaya dan kebutuhan alat berat untuk pemindahan tanah', *Jurnal Teknik Sipil Dan Arsitektur* **14**(18), 1–15.

Aydilek, A. H. and Arora, S. (2005), 'Class f fly ash amended soils as highway base materials', *Journal of Materials in Civil Engineering* **17**(6), 1–10.
URL: *https://doi.org/10.1061/(ASCE)0899-1561(2005)17:6(640)*

Bagheri, I., Kalhori, S. B., Akef, M. and Khormali, F. (2012), 'Effect of compaction on physical and micromorphological properties of forest soils', *American Journal of Plant Sciences* **03**(01), 159–163.
URL: *https://doi.org/10.4236/ajps.2012.31018*

Baloochi, H. (2022), Use of alternative materials in soil stabilization: mechanical and environmental aspects, Doctoral thesis report, Universitat Politècnica de Catalunya, UPC BarcelonaTech, Barcelona.

Bensoula, M., Bousmaha, M. and Missoum, H. (2022), 'Relative density influence on the liquefaction potential of sand with fines', *Revista de la Construcción* **21**(3), 692–702.
URL: *https://doi.org/10.7764/RDLC.21.3.692*

Briaud, J. L. (2013), *Geotechnical Engineering: Unsaturated and Saturated Soils*, second edition edn, John Wiley & Sons, New Jersey.

Chyliński, F. (2024), 'Microstructural assessment of pozzolanic activity of ilmenite mud waste compared to fly ash in cement composites', *Materials* **17**(11), 1–18.
URL: *https://doi.org/10.3390/ma17112483*

Cristelo, N., Glendinning, S. and Pinto, A. T. (2011), 'Deep soft soil improvement by alkaline activation', *Proceedings of the Institution of Civil Engineers - Ground Improvement* **164**(2), 73–82.
URL: *https://doi.org/10.1680/grim.900032*

Darwis (2018), *Dasar-Dasar Mekanika Tanah*, Pena Indis, Yogyakarta.

Di Sante, M., Khan, M. K., Calò, L., Fratalocchi, E. and Mazzieri, F. (2025), 'The combined use of fly ash and lime to stabilize a clayey soil: a sustainable and promising approach', *Geosciences* **15**(9), 1–17.
URL: *https://doi.org/10.3390/geosciences15090346*

Dissanayake, T. B. C. H., Senanayake, S. M. C. U. and Nasvi, M. C. M. (2017), 'Comparison of the stabilization behavior of fly ash and bottom ash treated expansive soil', *Engineer: Journal of the Institution of Engineers, Sri Lanka* **50**(1), 11–19.
URL: *https://doi.org/10.4038/engineer.v50i1.7240*

Dong, L., Cao, J. and Liu, X. (2022), 'Recent developments in sea-level rise and its related geological disasters mitigation: a review', *Journal of Marine Science and Engineering* **10**(3), 1–20.
URL: *https://doi.org/10.3390/jmse10030355*

Febrian, L., Susilo, A. J. and Setiawan, A. P. (2024), 'Analisis perubahan kuat geser pada tanah lempung dan pasir akibat penambahan fly ash tipe c', *JMTS: Jurnal Mitra Teknik Sipil* **4**(7), 1137–1144.
URL: *https://doi.org/10.24912/jmts.v7i4.30820*

Frempong, E. B. and Shukla, S. K. (2018), 'Stability analysis and design charts for a sandy soil slope supporting an embedded strip footing', *International Journal of Geo-Engineering* **9**(1), 1–23.
URL: *https://doi.org/10.1186/s40703-018-0082-2*

Golewski, G. L. (2022), 'The role of pozzolanic activity of siliceous fly ash in the formation of the structure of sustainable cementitious composites', *Sustainable Chemistry* **3**(4), 520–534.
URL: *https://doi.org/10.3390/suschem3040032*

Government of the Republic of Indonesia (2021), Peraturan pemerintah nomor 22 tahun 2021 tentang penyelenggaraan perlindungan dan pengelolaan lingkungan hidup, Technical report, Kementerian Sekretariat Negara, Jakarta.

Gunawan, G. and Nono (2019), 'Potensi pemanfaatan bahan limbah fly ash dan bottom ash untuk lapisan fondasi jalan semen (potential for utilization of fly ash and bottom ash waste materials for cement road foundation)', *Jurnal Jalan-Jembatan* **36**(1), 19–29.

Gupta, G., Sood, H. and Gupta, P. K. (2024), 'Economic and environmental assessment of industrial wastes stabilized clay and sand soil subgrades using experimental and theoretical approaches', *Construction and Building Materials* **422**(1), 1–55.
URL: *https://doi.org/10.1016/j.conbuildmat.2024.135787*

Herwandi, Marsudi and Aprianto (2017), Pengaruh gradasi dan kepadatan relatif (dr) terhadap nilai permeabilitas tanah pasir, Technical report, Universitas Tanjungpura, Pontianak.

Igwe, O. (2018), 'The combined effect of particle size distribution and relative density on the large strain behavior of sandy soils', *Geotechnical and Geological Engineering* **36**(2), 1037–1048.
URL: *https://doi.org/10.1007/s10706-017-0372-z*

Karthikeyan, K. R. and George, E. H. (2023), 'A review on effect of soil stabilization using alkali activated geopolymer', *Sustainability, Agri, Food and Environmental Research* **10**(10), 1–11.
URL: *https://doi.org/10.7770/safer-V10N1-art2463*

Keramatikerman, M., Chegenizadeh, A. and Nikraz, H. (2017), 'Experimental study on effect of fly ash on liquefaction resistance of sand', *Soil Dynamics and Earthquake Engineering* **1**(93), 1–6.
URL: *https://doi.org/10.1016/j.soildyn.2016.11.012*

Koester, J. P. and Tsuchida, T. (1988), Earthquake-induced liquefaction of fine-grained soils-considerations from japanese research, Technical report, Port and Harbor Research Institute, Yosaka.

Kolias, S., Kasselouri-Rigopoulou, V. and Karahalios, A. (2005), 'Stabilisation of clayey soils with high calcium fly ash and cement', *Cement and Concrete Composites* **27**(2), 301–313.
URL: *https://doi.org/10.1016/j.cemconcomp.2004.02.019*

Laia, B. (2015), 'Pengaruh kerapatan tanah pasir kali opak pleret yogyakarta terhadap potensi likuifaksi berdasarkan uji shaking table', *Jurnal Inersia* **7**(1), 40–49.

Legrans, R. R. (2016), 'Studi potensi likuifaksi berdasarkan uji penetrasi standar (spt) di pesisir pantai belang minahasa tenggara', *TEKNO* **14**(65), 37–48.
URL: *https://doi.org/10.35793/jts.v14i65.11924*

Lestari, P. (2022), Hubungan antara permeabilitas dengan diameter efektif (d10) pada tanah pasir di pantai padang, Bachelor thesis report, Universitas Andalas, Padang.

Mahvash, S., López-Querol, S. and Bahadori-Jahromi, A. (2017), 'Effect of class f fly ash on fine sand compaction through soil stabilization', *Heliyon* **3**(3), e00274.
URL: *https://doi.org/10.1016/j.heliyon.2017.e00274*

Marsindi, D., Simatupang, M. and Kadir, A. (2022), 'Pengaruh curing time dan derajat kejenuhan terhadap kuat tekan bebas dan kuat tarik belah pada campuran pasir dan fly ash', *Jurnal Ilmiah Teknik Sipil* **10**(3), 116–123.
URL: *https://doi.org/10.55679/jts.v10i3.31247*

Mawlood, Y., Salih, A., Hummadi, R., Hasan, A. and Ibrahim, H. (2021), 'Comparison of artificial neural network (ann) and linear regression modeling with residual errors to predict the unconfined compressive strength and compression index for erbil city soils, kurdistan-iraq', *Arabian Journal of Geosciences* **14**(485), 1–14.
URL: *https://doi.org/10.1007/s12517-021-06712-4*

Mehta, P. K. (2004), High-performance, high-volume fly ash concrete for sustainable development, Master thesis report, University of California, Berkeley.

Ministry of Public Works and Public Housing (PUPR) (2022), Peta deagregasi bahaya gempa indonesia untuk perencanaan dan evaluasi infrastruktur tahan gempa, Technical report, Direktorat Bina Teknik Permukiman dan Perumahan, Jakarta.

Misra, A. (1998), 'Stabilization characteristics of clays using class c fly ash', *Transportation Research Record: Journal of the Transportation Research Board* **1611**(1), 46–54.
URL: *https://doi.org/10.3141/1611-06*

Mohsen, M. O., Aburumman, M. O., Al Diseet, M. M., Taha, R., Abdel-Jaber, M., Senouci, A. and Abu Taqa, A. (2023), 'Fly ash and natural pozzolana impacts on sustainable concrete permeability and mechanical properties', *Buildings* **13**(8), 1–19.
URL: *https://doi.org/10.3390/buildings13081927*

National Standardization Agency of Indonesia (2008), Cara uji berat jenis tanah (sni 1964:2008), Technical report, BSN, Jakarta.
URL: *http://www.bsn.go.id*

National Standardization Agency of Indonesia (2012), Metode uji kuat tekan-bebas tanah kohesif (sni 3638:2012), Technical report, BSN, Jakarta.
URL: *http://www.bsn.go.id*

Noaman, M. F., Khan, M. A., Ali, K. and Hassan, A. (2022), 'A review on the effect of fly ash on the geotechnical properties and stability of soil', *Cleaner Materials* **6**(1), 1–14.
URL: *https://doi.org/10.1016/j.clema.2022.100151*

Nurdiyanto, T. D., Fatah, I. A. N. and Rochim, A. (2024), 'Pengaruh penambahan fly ash dan kapur pada tanah lempung ekspansif terhadap uji cbr', *Jurnal Ilmiah Sultan Agung* **3**(3), 208–218.

Osok, F. K., Simatupang, M. and Makmur, M. (2023), 'Penerapan fly ash sebagai bahan sementasi dalam pendekatan perbaikan tanah', *Jurnal Ilmiah Teknik Sipil* **11**(2), 97–103.

Pandian, N. S. (2004), 'Fly ash characterization with reference to geotechnical applications', *Journal of the Indian Institute of Science* **84**, 189–216.

Pangaribuan, E. A. S., Darmawati, A. and Budiyanto, S. (2020), 'Pertumbuhan dan hasil tanaman pakchoy pada tanah berpasir dengan pemberian biochar dan pupuk kandang sapi', *Agrosains: Jurnal Penelitian Agronomi* **22**(2), 72–78.
URL: *https://doi.org/10.20961/agsjpa.v22i2.42093*

Park, D. Y., Chang, I., Lee, M. and Cho, G. C. (2025), 'Enhancing soil liquefaction resistance and small-strain dynamic properties using cation-crosslinked biopolymer hydrogel', *Soil Dynamics and Earthquake Engineering* **190**, 1–12.
URL: *https://doi.org/10.1016/j.soildyn.2025.109212*

Pratiwi, D. S. (2020), 'Evaluasi perbaikan tanah menggunakan rapid impact compaction pada tanah berpotensi likuefaksi', *Jurnal Teknologi Ramah Lingkungan* **4**(2), 82–92.
URL: *https://doi.org/10.26760/jrh.v4i2.82-92*

Rahmayanti, R., Bahar, F. F. and Nuklirullah, M. (2023), 'Pemanfaatan dan pengaruh fly ash batu bara sebagai substitusi sebagian semen terhadap nilai kuat tekan bata ringan jenis cellular lightweight concrete (clc)', *Siklus: Jurnal Teknik Sipil* **9**(2), 218–228.
URL: *https://doi.org/10.31849/siklus.v9i2.11438*

Ruiz-Chávez, F. D. J., Gutiérrez-Villalobos, J. M. and Arroyo, H. (2022), 'Characterization of the relationship soil density and simple compression resistance of silty soils', *Revista de Ingeniería Mecánica* **6**(18), 15–20.
URL: *https://doi.org/10.35429/jme.2022.18.6.15.20*

Sakaguchi, A., Nishimura, T. and Kato, M. (2005), 'The effect of entrapped air on the quasi-saturated soil hydraulic conductivity and comparison with the unsaturated hydraulic conductivity', *Vadose Zone Journal* **4**(1), 139–144.
URL: *https://doi.org/10.2136/vzj2005.0139*

Santana, T., Gonçalves, J., Pinho, F. and Micaelo, R. (2021), 'Effects of the ratio of porosity to volumetric cement content on the unconfined compressive strength of cement bound fine grained soils', *Infrastructures* **6**(7), 1–19.
URL: *https://doi.org/10.3390/infrastructures6070096*

Sholihah, S. M., Hoesain, I. M. and Sulistyowati, T. (2019), 'Pengaruh variasi kedalaman muka air terhadap keruntuhan pondasi pada tanah pasir pantai dengan perkuatan anyaman bambu', *Spektrum Sipil* **6**(1), 69–77.
URL: *https://doi.org/10.29303/spektrum.v6i1.147*

Siddique, R. (2004), 'Performance characteristics of high-volume class f fly ash concrete', *Cement and Concrete Research* **34**(3), 487–493.
URL: *https://doi.org/10.1016/j.cemconres.2003.09.002*

Simatupang, M., Edwin, R. S., Sulha, Mustika, W., Putra, H. and Yanto, D. H. Y. (2022), 'Splitting tensile strength of fly ash-modified sand at various saturation and curing time', *Infrastructures* **7**(126), 1–16.
URL: *https://doi.org/10.3390/infrastructures7100126*

Simatupang, M., Mangalla, L. K., Edwin, R. S., Putra, A. A., Azikin, M. T., Aswad, N. H. and Mustika, W. (2020), 'The mechanical properties of fly-ash-stabilized sands', *Geosciences* **10**(132), 1–19.
URL: *https://doi.org/10.3390/geosciences10040132*

Temiz, C. (2022), Retracted: Scanning electron microscopy, *in* 'Electron Microscopy', IntechOpen.
URL: *https://doi.org/10.5772/intechopen.103956*

Transportation Research Board (1986), State of the art report 5: Reactions, properties, design, and construction, Technical report, National Academy Press, Washington DC.

Turan, C., Javadi, A. A. and Vinai, R. (2022), 'Effects of class c and class f fly ash on mechanical and microstructural behavior of clay soil—a comparative study', *Materials* **15**(5), 11–24.
URL: *https://doi.org/10.3390/ma15051845*

Turan, C., Javadi, A., Vinai, R., Shariatmadari, N. and Farmani, R. (2020), Use of class c fly ash for stabilization of fine-grained soils, *in* 'E3S Web of Conferences', Vol. 195, pp. 1–5.
URL: *https://doi.org/10.1051/e3sconf/202019506001*

Ulum, M. B. (2014), Karakteristik fisik dan kimia fly ash dari perusahaan ready mix beton dan limbah pabrik terhadap sifat mekanik pasta dan mortar, Bachelor thesis report, Institut Teknologi Sepuluh Nopember, Surabaya.

Upadhyay, A., Kamal, M., Pal, B. K. and Tripathy, D. P. (2007), Characterization and utilization of fly ash, Bachelor thesis report, National Institute Of Technology Rourkela, Orissa.

Vennapusa, C. S. R. and Eluru, A. (2025), 'Microstructural and mechanical evaluation of hvfac incorporating recycled plastic flakes and pozzolanic additives for environmental sustainability', *Environmental Challenges* **20**(1), 1–29.
URL: *https://doi.org/10.1016/j.envc.2025.101196*

Yadav, V. K., Yadav, K. K., Tirth, V., Jangid, A., Gnanamoorthy, G., Choudhary, N., Islam, S., Gupta, N., Son, C. T. and Jeon, B. H. (2021), 'Recent advances in methods for recovery of cenospheres from fly ash and their emerging applications in ceramics, composites, polymers and environmental cleanup', *Crystals* **11**(9), 1–20.
URL: *https://doi.org/10.3390/cryst11091067*

Yazici, E. and Unsever, Y. S. (2024), 'Investigation of cement and fly ash on the improvement of fine sand soil', *Applied Sciences* **14**(7), 1–10.
URL: *https://doi.org/10.3390/app14072908*

Zen, K., Jeng, D., Hsu, J. and Ohyama, T. (1998), 'Remedial measures for reclaimed land by premixing method', *Soil Mechanics and Foundation Engineering* **42**(3), 37–42.

Zeybek, A. and Madabhushi, G. S. P. (2017), 'Durability of partial saturation to counteract liquefaction', *Proceedings of the Institution of Civil Engineers: Ground Improvement* **170**(2), 102–111.
URL: *https://doi.org/10.1680/jgrim.16.00025*

Zhang, H., Ren, H., Mu, C., Wu, X., Huang, K. and Wang, F. (2023), 'Experiment study on the influence of density and confining pressure on triaxial shear properties of calcareous sand', *Materials* **16**(4), 1–14.
URL: *https://doi.org/10.3390/ma16041683*